



HAL
open science

Experimental validation of off-line energy management strategies applied to a hybrid FC/SC system

Qi Jiang, Olivier Béthoux, Florence Ossart, Éric Berthelot, Claude Marchand

► **To cite this version:**

Qi Jiang, Olivier Béthoux, Florence Ossart, Éric Berthelot, Claude Marchand. Experimental validation of off-line energy management strategies applied to a hybrid FC/SC system. ELECTRIMACS 2017, Jul 2017, Toulouse, France. hal-01693644

HAL Id: hal-01693644

<https://hal.science/hal-01693644>

Submitted on 11 Mar 2020

HAL is a multi-disciplinary open access archive for the deposit and dissemination of scientific research documents, whether they are published or not. The documents may come from teaching and research institutions in France or abroad, or from public or private research centers.

L'archive ouverte pluridisciplinaire **HAL**, est destinée au dépôt et à la diffusion de documents scientifiques de niveau recherche, publiés ou non, émanant des établissements d'enseignement et de recherche français ou étrangers, des laboratoires publics ou privés.

EXPERIMENTAL VALIDATION OF OFF-LINE ENERGY MANAGEMENT STRATEGIES APPLIED TO A HYBRID FC/SC SYSTEM

Qi JIANG, Olivier BETHOUX, Florence OSSART, Eric BERTHELOT, Claude MARCHAND

GeePs | Group of Electrical Engineering – Paris
UMR CNRS 8507, CentraleSupélec, Univ Paris-Sud, Sorbonne Universités, UPMC Univ Paris 06
3, 11 rue Joliot-Curie, Plateau de Moulon F-91192 Gif-sur-Yvette CEDEX
e-mail: florence.ossart@geeps.centralesupelec.fr

Abstract – The energy management of a hybrid fuel cell / supercapacitor system is studied, both in simulation and on a test bench, for experimental validation. This system can be used to power a urban electric scooter. Two off-line energy management strategies are implemented and compared to control the power split between the fuel cell and the supercapacitor: Pontryaguine minimum principle (PMP) and dynamic programming. In the case of PMP, time evolution of the co-state is accounted for, and operational constraints on the supercapacitor state of charge are included. Simulation and experimental results agree very well, which validates the system model and the implementation of the control strategies on the real system. This work will be used as a basis to develop online strategies.

Keywords – fuel cell systems, energy management, optimal control, dynamic programming, Pontryagin minimum principle.

1. INTRODUCTION

Fuel cell electric vehicles (FCEVs) are considered as a promising alternative for fossil fuel economy and greenhouse gas emission reduction because of their low environmental effects and high efficiency, in particular if the fuel H_2 is produced through electrolysis using renewable energy sources. FCEVs possess an electrochemical power source (the FC) and an energy storage system such as a supercapacitor (SC) or a battery pack [1]. Currently, SC are chosen because they have a higher specific power than batteries and a longer lifetime in terms of number of charge/discharge cycles [2]. This combination of two power sources (FC and SC) allows to improve the global efficiency of the system over a given trip thanks to two mechanisms: the FC can be operated at a good efficiency whatever the effective power delivered to the vehicle, and kinetic energy can be recovered during braking. For these purposes, an efficient energy management strategy is needed, in order to determine an appropriate power split between the FC and the SC, and to minimize the total H_2 consumption over a given driving cycle, while meeting the driver's power demand and satisfying operating constraints.

In the case of perfectly controlled conditions (design, sizing or test), the driving cycle is fully known in advance and two well-known optimal control methods are available: Pontryagin's minimum principle (PMP) [3] and dynamic programming (DP) [4]. PMP is easy to implement

and fast, but does not allow to account for interval constraint on the state variable. On the other hand, DP is a more cumbersome method, but is more robust and naturally handles state variables constraints when needed.

Whatever the chosen method, its performances rely on the accuracy of the system model and on the quality of the implementation in the actual system. The present paper addresses this issue in the case of a hybrid FC/SC system suitable to power a urban scooter. The system components are modelled from experimental characteristics and both DP and PMP algorithm are tested on the test bench. Comparison between simulation and experiments shows the accuracy of the model and the ability of the implemented strategies to actually minimize the system H_2 consumption. In real life, the driving cycle is not known ahead of time and so-called online energy management strategies are needed. The present work is intended to be a starting point to study such strategies.

The paper is organized as follows. The FC/SC system and the models used are described in Section 2. The PMP and DP optimal management strategies are presented in Section 3. Simulation and experimental results are discussed in Section 4. Their good agreement shows that the model is accurate and that the energy strategies are properly implemented on the test bench. Finally, the paper is concluded in Section 5.

2. FC/SC SYSTEM MODELING

2.1. SYSTEM PRESENTATION

The present work deals with the hybrid FC/ SC system shown in Fig.1, suitable to power a urban electric scooter.

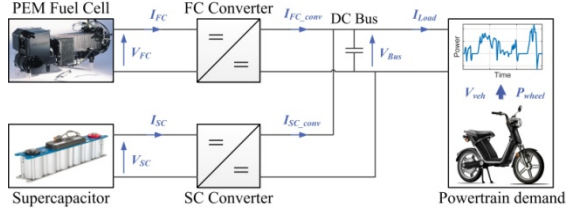


Fig. 1. FC/SC hybrid system model

The scooter electric motor is fed by a DC electric bus, connected to the FC through a unidirectional boost converter and to the SC pack through a bidirectional converter. The experimental test bench, shown on Fig. 2, does not include the electric motor. The DC bus load P_{load} is directly the scooter drive wheel power demand P_{wheel} ,

$$P_{load} = V_{Bus} \cdot I_{load} = P_{wheel} \quad (1)$$

where P_{wheel} is calculated using the motion equation of the scooter and the driving cycle, as explained in Section 2.5.

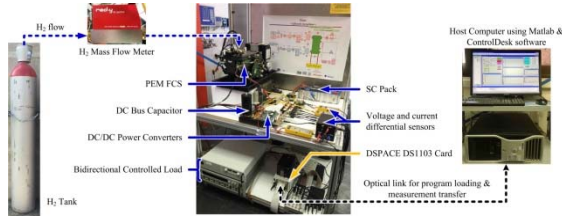


Fig. 2. Experimental setup.

2.2. FUEL CELL

The main power source of the system is a 1.2 kW proton exchange membrane FC, modeled using its static V-I characteristic [5]. The hydrogen chemical power P_{ch} is expressed as a function of the output electric power P_{FC} by fitting experimental data with a fourth-order polynomial. Then the hydrogen consumption rate is determined by (2), where HHV is the high heating value of hydrogen.

$$\dot{m}_{H_2} = \frac{P_{ch}(P_{FC})}{HHV} \quad (2)$$

Fig. 3 shows the measured FCS efficiency and the modeled one, using (2). The FC model gives a maximum efficiency for an output power around 300 W.

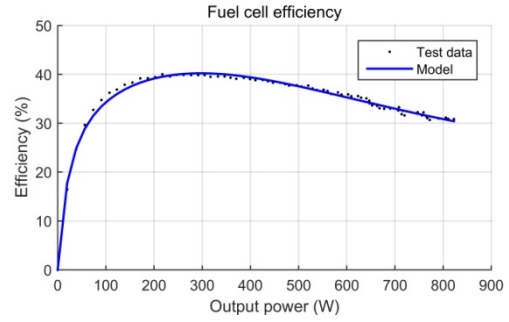


Fig. 3. FC efficiency versus output power

2.3. SUPERCAPACITOR

The SC stack is modeled as a RC circuit in parallel with an internal leakage current source which represents the losses due to active cell balancing technology used in SC packs [6], as shown in Fig. 4.

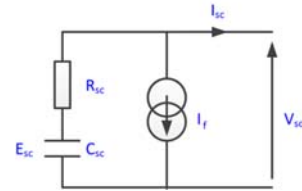


Fig. 4. SC stack model

For a given output current I_{SC} and output voltage V_{SC} , the internal capacitor is charged ($P_{int} < 0$) or discharged ($P_{int} > 0$) according to formula (3).

$$P_{int} = R_{SC} \cdot (I_{SC} + I_f)^2 + V_{SC} \cdot (I_{SC} + I_f) \quad (3)$$

The leakage current I_f is expressed as a quadratic function of V_{SC} obtained by fitting experimental data measured in no load condition.

2.4. DC/DC CONVERTERS

The FC/SC systems needs two DC/DC converters, both modeled as ideal converters connected in parallel with leakage current sources that represent the converter internal losses. The losses are accurately measured using an opposition method described in [7].

The output current of the FC converter can be expressed by (4), where I_f is the leakage current obtained by fitting the experimental data with a quadratic function of I_{FC} .

$$I_{FC_conv} = \frac{V_{FC} I_{FC}}{V_{Bus}} - I_f \quad (4)$$

The SC converter is modeled the same way.

2.5. DRIVING CYCLE AND POWER DEMAND

The present study is based on the World Motorcycle Test Cycle (WMTC), dedicated to low power motorcycles [8], and shown in Fig. 5.

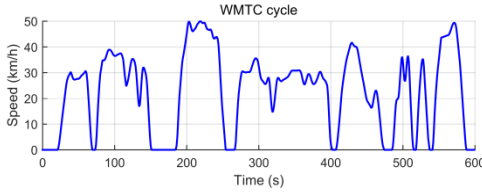


Fig. 5. WMTC driving cycle profile

The power demand corresponding to this speed profile, is determined using the motion equation of the vehicle:

$$P_{wheel} = \left(\frac{1}{2} \rho_{air} A C_d v_{veh}^2 + \mu_r M g + M a \right) v_{veh} \quad (5)$$

where ρ_{air} is density of air; A is the reference area; C_d is the drag coefficient; μ_r is the rolling resistance coefficient; M is the vehicle mass; g is the gravitational acceleration; a is the vehicle acceleration. The power profile corresponding to the WMTC cycle is shown later, in Fig.6.

3. OPTIMAL ENERGY MANAGEMENT

The purpose of optimal power management is to determine the best instantaneous power split between the FC and the SC in order to minimize the fuel consumption over the whole driving cycle, while meeting the driver's power demand and satisfying operating constraints. The system state is represented by the energy stored in the SC, E_{SC} , whereas P_{FC} is chosen as control variable. P_{load} can then be considered as an external disturbance. For easier writing, E_{SC} , P_{FC} and P_{load} will be respectively denoted x , u and w hereafter.

The problem is defined by (6) - (9), where J is the total H_2 consumption over the considered time interval. Since the energy is provided solely by the fuel, the consumption should be calculated with equal initial and final state. In between, the SC either stores or provides power to adjust the FC working point and recover braking energy.

$$\text{Minimize } J = \int_{t_0}^{t_f} P_{ch}(u(t)) dt \quad (6)$$

$$\text{subject to } \dot{x}(t) = -P_{int} = f(u(t), x(t), w(t)) \quad (7)$$

$$x(t_f) = x(t_0) = x_{ref} \quad (8)$$

$$x_{min} \leq x(t) \leq x_{max} \quad (9)$$

In the case of off-line optimization, the driving cycle is fully known in advance and two mathematical approaches can be applied to solve the problem: Pontryagin's minimum principle (PMP) and dynamic programming (DP).

3.1. PONTRYAGIN'S MINIMUM PRINCIPLE

PMP applies when the constraint (9) is left out. It uses the Hamiltonian function defined by (10), where $p(t)$ is the co-state related to the dynamic equation (7) [9].

$$H(p, u, x, w) = P_{ch}(u) - p(t) f(u, x, w) \quad (10)$$

PMP states that if u^* is the solution of problem (6) - (8), there exists a function $p(t)$, whose dynamics is governed by (11), and such that (12) and (8) hold.

$$\forall t \in [t_0, t_f] \quad \frac{dp}{dt}(t) = -\frac{\partial H}{\partial x}(x, u, p, w) \quad (11)$$

$$\forall t \in [t_0, t_f] \quad \frac{\partial H}{\partial u}(x, u, p, w) = 0 \quad (12)$$

In the case of battery storage, it is common to neglect the influence of the battery state of charge on its open source voltage and internal resistance, and hence to consider $p(t)$ as a constant [10]. In the present case, this simplification does not hold because the state variation $\dot{x} = P_{int}$ depends on the output voltage, which in turn depends on the state $x = E_{SC}$. Hence, the partial derivative equation (11) is solved in order to calculate the co-state evolution with time.

In our problem, it is important that the constraint (9) is fulfilled at all times to ensure safe operation of the SC. Hence, the algorithm proposed in [11] is applied: whenever the constraint (9) is violated, the cycle is split in consecutive sub-cycles and intermediary constraints are added to keep the state trajectory within the allowed boundaries. The other method which has been implemented, namely DP, naturally accounts for this constraint and results will be compared.

3.2. DYNAMIC PROGRAMMING

DP is a multi-stage decision-making process which applies well to the optimization of cumulative costs in dynamic systems, such as the present one [12]. It requires the problem to be discretized in time and state. Let us denote respectively 0 and N the indexes of the initial and final time steps, $x_k = E_{SC}(t_k)$, $u_k = P_{FC}(t_k)$ and $w_k = P_{load}(t_k)$.

The discretized problem is given by (13) - (16).

$$\text{Minimize } J = \sum_{k=0}^{N-1} P_{ch}(u_k) \cdot \Delta t \quad (13)$$

$$\text{subject to } x_{k+1} = x_k + f(u_k, x_k, w_k) \cdot \Delta t \quad (14)$$

$$x_0 = x_N = x_{ref} \quad (15)$$

$$x_{min} \leq x_k \leq x_{max} \quad (16)$$

A so-called cost-to-go function, denoted $J_k(x)$, is defined at each time step t_k . It corresponds to the minimum cost that can be obtained by optimal

control from a given intermediary state $x_k = x$ to the final state x_N . This cost is calculated backwards, starting from (17) and applying the recursive process (18) - (19), where $u_k^*(x)$ denotes the optimal control at time t_k as a function of the current system state $x_k = x$.

- Initialization: at $k = N - 1$

$$J_{N-1}(x_{N-1}) = P_{ch}(u_{N-1}) \cdot \Delta t \quad (17)$$

- Backward iterative process: from $k = N - 2$ to $k = 0$

$$J_k(x) = \min_u \{P_{ch}(u) \cdot \Delta t + J_{k+1}(x + f(x, u, w_k))\} \quad (18)$$

$$u_k^*(x) = \operatorname{argmin}_u \{P_{ch}(u) \cdot \Delta t + J_{k+1}(x + f(x, u, w_k))\} \quad (19)$$

At the end of the backward process, $J_0(x)$ represents the minimum fuel consumption which can be obtained starting from the initial state $x_0 = x$. The optimal control policy $\{u_k^*\}_{0 \leq k \leq N-1}$ and state trajectory $\{x_k^*\}_{0 \leq k \leq N-1}$ are rebuilt by a forward process.

PMP and DP are equivalent when the Hamiltonian function is convex, and the co-state is linked to the cost-to-go function according to (20) [13]. This relationship will be used to assess the quality of the results of both methods.

$$p_k = -\frac{dJ_k}{dx}(x = x^*) \quad (20)$$

4. SIMULATION RESULTS AND EXPERIMENTAL VALIDATION

PMP and DP were implemented both in simulation and for the open-loop control of the FC/SC hybrid system. For a given load profile, the optimal control is determined by simulation for each tested algorithms. Then, it is applied to the fuel cell, in order to experimentally verify the method performance for the real system.

Two versions of PMP algorithm have been tested: a simplified one, referred to as PMPc, where the co-state p is kept constant, and the optimal one, referred to as PMPv, where the co-state time evolution is calculated using (13).

The different strategies were applied with the load profile calculated from the WMTC driving cycle and shown in Fig. 6.

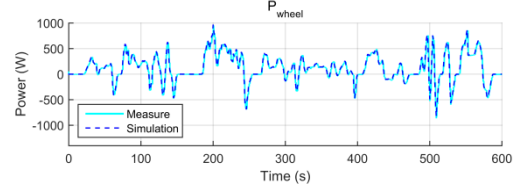


Fig. 6. Load power profile

Several experimental runs were performed, in order to test the repeatability of the process, which is good. As an example, Table I reports the fuel consumption J , and the difference between the initial and final SC state, for two experimental runs.

Table I. WMTC cycle results

Strategy	J (10^{-1} g/km)			Δx (%)		
	sim	exp1	exp2	Sim	exp1	exp2
PMPc	3.72	3.84	3.87	-0.1	0.7	2.1
PMPv	3.70	3.73	3.72	0.2	-2.3	-1.4
DP	3.70	3.74	3.76	0	-2.5	-5.1

For the three strategies, the difference between the measured and calculated values is less than 3% for the fuel consumption and 5% for the final state-difference. This small discrepancy validates the accuracy of the FC/SC system model and the correctness of the strategy implementation.

As expected, PMPv and DP give identical consumptions, but one notices that PMPc is only slightly above: accounting for the co-state evolution does not seem worth the effort, at least for the considered example.

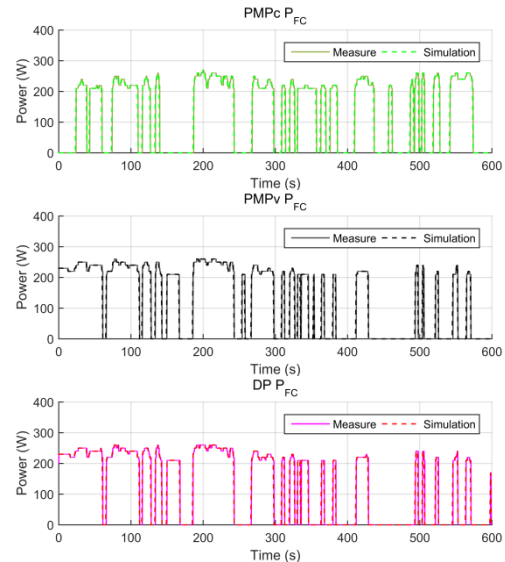


Fig. 7. Control profile comparison

The control profiles found by the three considered strategies are plotted in Fig.7. They are very similar and show that the FC is operated mostly around 250 W, at its best efficiency. The profiles calculated by PMPv and DP differ only in some isolated points, and this is due to the fact that the Hamiltonian function defined by (10) sometimes has two local minima, with almost equal values. The result is then

sensitive to numerical noise, which leads to different commands. This fact was also mentioned and analysed in [14].

Fig.8 gives an example of hydrogen consumption rate curve, obtained with DP. The fuel consumption rate follows the FC output power, and the good agreement between simulation and experiments illustrates the quality of the FC model.

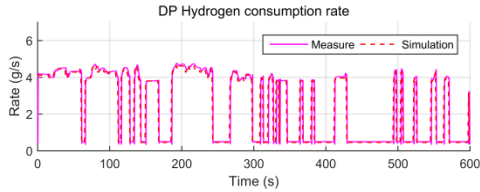


Fig. 8. Fuel consumption rate with DP strategy

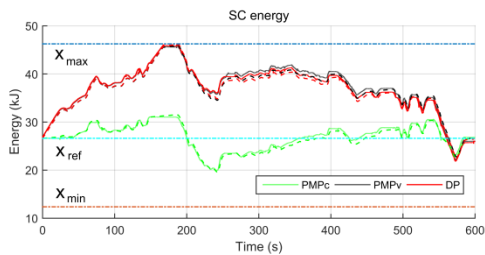


Fig. 9. SC state evolution : full and dashed lines respectively correspond to simulation and experiments

The SC state evolution curves $x(t)$ associated to the different control strategies are plotted and compared in Fig.9. Both DP and PMPv give the same trajectory, which follows the upper state limit $x_{max} = 46.2 \text{ kJ}$ between $t = 168 \text{ s}$ and $t = 188 \text{ s}$. A closer look to the DP and PMPv trajectories shows that they actually hit the upper limit only at $t = 188 \text{ s}$, when the wheel power exceeds the optimal efficiency FC operating point and that the SC energy is used to keep the FC working around this point. The agreement between the state trajectories predicted using PMPv and DP shows the effectiveness of the algorithm used to account for the interval constraint on the SC state. PMPc state trajectory is a more "charge-sustaining" one, confined around the reference state $x_{ref} = 26.6 \text{ kJ}$. This trajectory is sub-optimal, but the over-consumption is small.

The co-state values calculated by PMPc and PMPv are shown in Fig.10. When its time dependence is accounted for, the co-state is a decreasing function, except at time $t = 188 \text{ s}$, when the constraint $x(t) \leq x_{max}$ is activated. At this point, a local discontinuity takes place, resulting from the split of the drive profile in two sub-profiles with an intermediate constraint. In the case of PMPc, the co-state is assumed to be constant and an average value is obtained. One notices that neglecting the time dependence of the co-state does not affect very much the consumption, but much more the SC state

trajectory. At the beginning of the WMTC cycle, the PMPc co-state value is smaller than the one of PMPv, and less energy is stored in the SC. At the end of the driving cycle, the opposite happens.

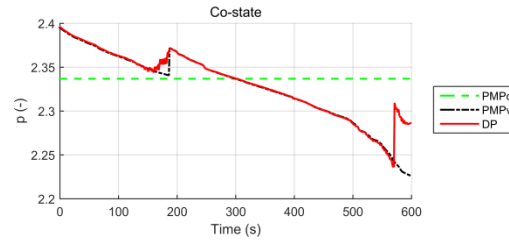


Fig. 10. Co-state value versus time

In the case of DP, the co-state can also be calculated by applying (20) to the cost-to-go matrix. The discrete value of the co-state at time t_k is calculated using (21).

$$p_k = -\frac{J_k(x_{k+1}^*) - J_k(x_k^*)}{2 \cdot \Delta x} \quad (21)$$

The values found using DP match very well the ones calculated directly by PMPv, except when the state trajectory follows the border of the reachable state region, shown on Fig. 11. During these time intervals, numerical noise affects the numerical derivation of J_k .

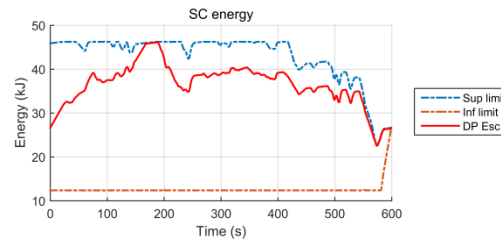


Fig. 11. State evolution obtained by DP

5. CONCLUSIONS

The energy management of a fuel cell system coupled to a supercapacitor energy storage system has been studied, both in simulation and on a test bench. This system can be used to power a urban FC scooter.

The system was modelled and two off-line energy management methods have been used : PMP and DP. PMP was implemented both with a constant and a variable co-state, and constraint on the state limitation was included.

Simulation and experimental results agree very well, which validates the system model and the implementation of the control strategies. It is found that accounting for the co-state time evolution may not be necessary: the global consumption is very close to the optimal one. More cycles should be tested to assess this result.

In real world, however, the driving cycle cannot be known in advance and so-called on-line energy management strategies are needed. In work underway, the model validated here is used as a basis to develop such strategies, and the off-line results provide reference consumption in order to assess the online strategies.

REFERENCES

- [1] N. SamExp, Fuel cell technology: reaching towards commercialization, Springer Science & Business Media, 2006.
- [2] Q. Li, W. Chen, Z. Liu, M. Li, L. Ma, Development of energy management system based on a power sharing strategy for a fuel cell-battery-supercapacitor hybrid tramway, *J. Power Sources*. 279 (2015) 267–280.
- [3] N. Kim, S. Cha, H. Peng, Optimal Control of Hybrid Electric Vehicles Based on Pontryagin's Minimum Principle, *IEEE Trans. Control Syst. Technol.* 19 (2011) 1279–1287. doi:10.1109/TCST.2010.2061232.
- [4] M. Ansarey, M.S. Panahi, H. Ziarati, M. Mahjoob, Optimal energy management in a dual-storage fuel-cell hybrid vehicle using multi-dimensional dynamic programming, *J. Power Sources*. 250 (2014) 359–371.
- [5] M. Hilaret, M. Ghanes, O. Béthoux, V. Tanasa, J.-P. Barbot, D. Normand-Cyrot, A passivity-based controller for coordination of converters in a fuel cell system, *Control Eng. Pract.* 21 (2013) 1097–1109.
- [6] D. Linzen, S. Buller, E. Karden, R.W. De Doncker, Analysis and evaluation of charge-balancing circuits on performance, reliability, and lifetime of supercapacitor systems, *IEEE Trans. Ind. Appl.* 41 (2005) 1135–1141.
- [7] F. Forest, J.J. Huselstein, S. Faucher, M. Elghazouani, P. Ladoux, T.A. Meynard, F. Richardeau, C. Turpin, Use of opposition method in the test of high-power electronic converters, *IEEE Trans. Ind. Electron.* 53 (2006) 530–541.
- [8] T.J. Barlow, S. Latham, I.S. McCrae, P.G. Boulter, A reference book of driving cycles for use in the measurement of road vehicle emissions, TRL Publ. Proj. Rep. (2009).
- [9] D.E. Kirk, Optimal control theory: an introduction, Dover Publications, 2004
- [10] Q. Jiang, F. Ossart, C. Marchand, Real-time HEV energy management strategies, Symposium de Genie Electrique (2016).
- [11] F. Odeim, J. Roes, L. Wülbeck, A. Heinzl, Power management optimization of fuel cell/battery hybrid vehicles with experimental validation, *J. Power Sources*. 252 (2014) 333–343.
- [12] D.P. Bertsekas, Dynamic programming and optimal control, 3rd edition, Athena Scientific, 2005.
- [13] F. H. Clarke, and R. B. Vinter, "The relationship between the maximum principle and dynamic programming," *SIAM J. Contr. Optim.*, vol.25, no.5, pp.1291-1311, 1987.
- [14] S. Delprat, and T. Hofman, "Hybrid Vehicle Optimal Control: Linear Interpolation and Singular Control," in *IEEE-VPPC*, Coimbra, 2014, pp.1-6.